Communication

Organic Janus Microspheres: A General Approach to All-Color Dual-Wavelength Microlasers

Cong Wei, Yuxiang Du, Yingying Liu, Xianqing Lin, Chuang Zhang, Jiannian Yao, and Yong Sheng Zhao

J. Am. Chem. Soc., **Just Accepted Manuscript** • DOI: 10.1021/jacs.9b00362 • Publication Date (Web): 20 Mar 2019

Organic Janus Microspheres: A General Approach to All-Color Dual-Wavelength Microlasers

Cong Wei,[†,‡] Yuxiang Du,[†,§] Yingying Liu,[†,§] Xianqing Lin,[†,§] Chuang Zhang,[†,§] Jiannian Yao,[†,§] and Yong Sheng Zhao*,[†,§]

[†]Key Laboratory of Photochemistry, Institute of Chemistry, Chinese Academy of Sciences, Beijing 100190, China.

[‡]College of Materials Science and Engineering, Zhengzhou University, Zhengzhou 450001, China

[§]University of Chinese Academy of Sciences, Beijing 100049, China.

Supporting Information Placeholder

ABSTRACT: We propose a general approach for the achievement of dual-wavelength organic microlasers in amphiphilic Janus resonators, where hydrophilic and hydrophobic dyes can be spatially separated via the polarity driven encapsulation. Low-threshold dual-wavelength lasing was successfully obtained in a single Janus particle with well-modulated output. This universal approach enables to flexibly design the lasing wavelength of the Janus microlasers in the full visible spectrum by systematically altering the encapsulated laser dyes. Our findings demonstrate a promising route to the photonic integration at micro/nanoscale that may lead to the innovation of concepts and device architectures for multifunctional optoelectronic applications.

Generating multicolor laser in a single compact system is crucial for biological labeling,[1] full-color laser display,[2] multichannel optical communication,[3] etc. The ever-increasing demand for wide display color gamut and high-throughput photonic devices calls for nanoscale multi-wavelength coherent light sources capable of emitting across the full visible spectrum.[4,5] Till now, multi-wavelength micro/nanolasers were realized mainly through integrating gain media with different bandgaps on a single device, where the lasing wavelengths correspond to the bandgaps of the respective materials.[6-8] Due to the absorption of short-wavelength emission by the narrow-gap material, lasing in the high-energy region is severely suppressed.[9,10] Spatially separating different gain materials in side-by-side geometries can minimize the absorption loss,[11-13] demonstrating an alternative solution to this problem.[14-16] Most of these composite cavities were constructed from inorganic lateral heterostructures, which requires overcoming the intrinsic difficulties in achieving epitaxial growth of the mismatched materials with different emissions, and thus limits the accessible spectral range of multi-wavelength lasing.

Janus microparticles, whose surfaces have two distinct physical properties, allow two different properties to occur on the same particle.[17-19] Among them, organic polymer Janus particles are typical representatives, with one-half of each particle composed of hydrophilic groups and the other half hydrophobic ones.[20,21] Based on the principle of like dissolves like, organic laser dyes with distinct polarities can be selectively encapsulated into the two hemistructures of a single Janus particle,[22-25] which will result in a typical side-by-side cavity geometry, providing a versatile approach to spatially separating the gain materials. Moreover, the high compatibility enable to spatially incorporate various gain media,[26,27] which would in principle provide a universal and robust strategy to construct dual-color microlasers with lasing wavelengths tunable within the entire visible region. Nevertheless, this is still limited by the synthesis of Janus microparticles with tunable compositions above the diffraction limit that can provide necessary feedback for lasing.

In this work, we report the general synthesis of fluorescent Janus microstructures for dual-wavelength lasers, where the two sides of each isotropic particle can be distinctively doped with hydrophilic and hydrophobic dyes. Low threshold dual-wavelength lasing was achieved in a single Janus particle and the lasing performance was highly dependent on the Janus structure, providing an effective modulation of the output signals. This approach is applicable for all hydrophilic and hydrophobic organic dyes, and the emission color of the Janus lasers was preliminarily tuned from blue-pink to green-orange by systematically altering the encapsulated dyes, showing tremendous potential to the design and fabrication of dual-wavelength lasers in all-color region. The results are anticipated to expand the application range of Janus nanomaterials, and provide helpful enlightenment for the optoelectronic integration in compact systems.

The fabrication of dye doped dual-color fluorescent Janus particles is illustrated in Figure 1a. According to the minimum Gibbs free energy criterion, guest laser dye molecules can be well dispersed in the host matrix if their interfacial energy ($\gamma_{H\text{-}G}$) is smaller than the entropy increment ($T\Delta S$) induced by the mixing ($\Delta G=\gamma_{H\text{-}G}-T\Delta S$); otherwise they will self-separate at the thermodynamic equilibrium state.[28] Thus, the hydrophilic part of the amphiphilic Janus microsphere will selectively encapsulate hydrophilic dyes, while its hydrophobic counterpart prefers hydrophobic molecules, forming an ideal heterogeneously luminescent microstructure for the achievement of dual-wavelength lasing via the whispering-gallery-mode (WGM) resonance.[29] Polystyrene (PS) and poly (methyl methacrylate) (PMMA), with different polarities, were selected as

the matrix materials to create Janus microlasers. The Janus structures were obtained by inducing phase separation of PS/PMMA within the micrometer-sized emulsion droplets (see Supporting Information). 1,4-Bis(α-cyano-4-diphenylaminostyryl)-2,5-diphenylbenzene (CNDPASDB, hydrophobic) and rhodamine-101 (Rh101, hydrophilic), with different emission and polarity (Figure S1), were adopted to provide optical gain for the operation of dual-wavelength laser.

In a typical preparation (Figure 1b), well mixed CNDPASDB/Rh101/PMMA/PS/CH_2Cl_2 solution was first added into the cetyltrimethylammonium bromide (CTAB) aqueous solution to form an oil-in-water emulsion. Hydrophobic CH_2Cl_2 solution was subsequently encapsulated into the hydrophobic interior of the CTAB micelles under vigorous stirring .[30,31] With the evaporation of CH_2Cl_2, spherical droplets consisting of PS and PMMA blends underwent phase separation to form Janus microspheres. According to the scheme in Figure 1a, hydrophobic CNDPASDB molecules prefer to be embedded into the nonpolar PS-rich hemispheres, while the hydrophilic Rh101 molecules will be dispersed in the polar PMMA matrix. The spatially selective doping behavior (Figure S2) drove the formation of the final dual-color Janus microspheres.

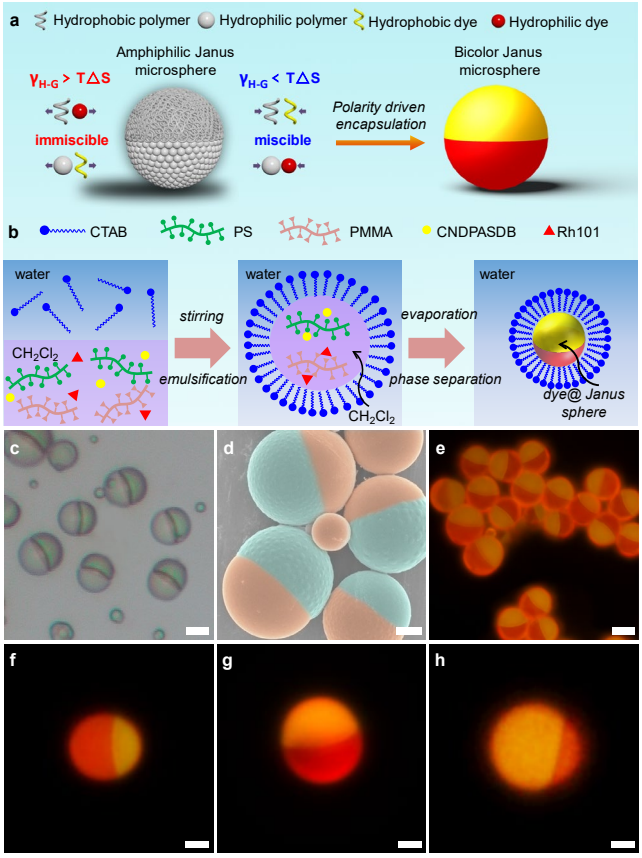

Figure 1. (a) Scheme for the design of Janus microspheres with dual-color emission. (b) Illustration for the synthesis of the dual-color Janus microspheres. (c) Optical microscopy images of the Janus microspheres. Scale bar: 5 μm. (d) SEM image of the Janus microspheres. Scale bar: 2 μm. (e) PL image of the CNDPASDB-Rh101 doped Janus microspheres. Scale bar: 5 μm. PL images of the CNDPASDB-Rh101 doped Janus microspheres obtained from various PS:PMMA weight ratios: (f) 3:4; (g) 1:1; (h) 4:3. Scale bars: 2 μm.

The spherical Janus geometry was confirmed by optical microscopy and SEM images (Figure 1c-d). A clear boundary was observed between the two hemispheres, which can be distinguished by their distinct surface morphologies, with one side being very smooth while the other slightly rough. The diameter of the Janus spheres is in direct proportion to the size of the micelles, which should strongly depend on the interfacial tension between water and CH_2Cl_2. The interfacial tension would increase with increasing amount of added polymer blends, generating larger micelles with smaller specific surface areas to reduce the interfacial energy of the whole system. This is exactly what we have observed from the controlled experiments, where the diameter of the Janus spheres was finely tuned from 3 to 15 μm through increasing the concentration of PS-PMMA blends (Figure S3). Furthermore, by altering the weight ratio of PMMA:PS, we were able to modulate the size ratio between the two hemispheres. As shown in Figure S4, the rough segment of the obtained Janus spheres became larger with increasing PS content. Therefore, we can identify that the side with rough surface is the PS-rich phase, while the smooth hemispheres are composed of PMMA-rich phase.

Under UV excitation, yellow and red fluorescence emissions were respectively observed from the two hemispheres (Figure 1e). Figure S5 shows the spatially resolved PL spectra collected from the two hemispheres in a single particle. which indicate the CNDPASDB emission dominates the spectrum collected from the left part, whereas the Rh101 dominates that from the right. The relative size of the CNDPASDB section increased with the increase of added PS, while the Rh101-dominant section was positively correlated to the added PMMA (Figure 1f-h). This further testifies that hydrophobic CNDPASDB molecules prefer to be embedded into the nonpolar PS-rich phase, while hydrophilic Rh101 molecules prefer to be incorporated into the polar PMMA. This discriminative doping behavior of laser dyes provides a general access to the side-by-side coupled optical microcavities.

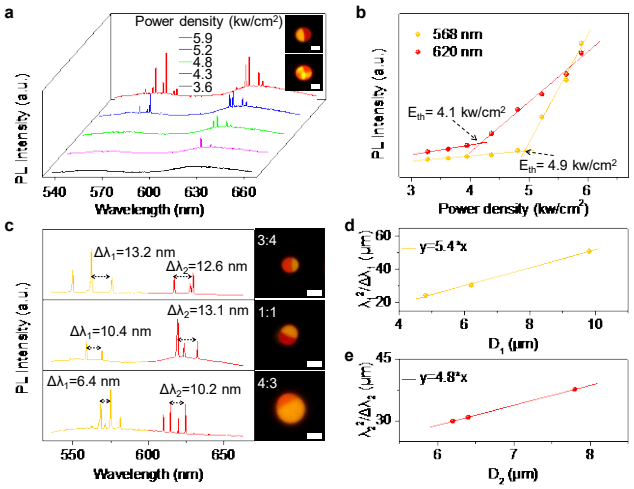

Figure 2. (a) PL spectra of a typical CNDPASDB-Rh101 doped Janus microsphere as a function of pump energy. Inset: PL images of the microsphere excited with UV light (top) and focused laser (bottom). Scale bars: 5 μm. (b) Power dependent

intensity for the CNDPASDB and Rh101 lasing. (c) PL spectra of the CNDPASDB-Rh101 doped Janus microspheres with different PS:PMMA ratios. Insets: corresponding PL images. Scale bars: 5 μm. (d) Relationship between $\lambda_1^2/\Delta\lambda_1$ and the diameter of the PS-rich hemisphere at CNDPASDB emission. (e) Relationship between $\lambda_2^2/\Delta\lambda_2$ and the diameter of the PMMA-rich hemisphere at Rh101 emission.

When a Janus microsphere was excited with a focused laser beam (Figure S6), bright emissions with distinct colors were separately obtained from the two hemispheres (Figure 2a, inset), indicating that the Janus geometry can effectively minimize the absorption loss of the short-wavelength emission. Figure 2a shows the PL spectra of a representative Janus microsphere pumped with increasing power. At a low pumping power, two broad bands with peak wavelengths at 560 and 630 nm appeared, consistent with the emissions of CNDPASDB and Rh101, respectively. When the power was increased to 4.3 kw/cm², sharp peaks with FWHM of ~0.5 nm started to emerge at Rh101 emission. When the pumping power was further elevated to 5.2 kw/cm², the intensity of the peaks at Rh101 emission strongly increased; meanwhile, new sharp lines emerged from the CNDPASDB band, and a dual-color laser was achieved. Figure 2b depicts the power-dependent intensity for the lasing at 568 and 620 nm, exhibiting two thresholds, 4.1 and 4.9 kw/cm², respectively. This is resulted from the transition from spontaneous to stimulated emissions of the two dyes.

The lasing spectra of the Janus microspheres with different diameters were characterized (Figure S7a) to study the microcavity effects. For WGM-type resonance, the mode spacing, $\Delta\lambda$, and the diameter, D, should satisfy the equation $\lambda^2/\Delta\lambda=n\pi D$, where λ is the resonance wavelength and n is the group refractive index.[32] Figure S7b-c plots $\lambda^2/\Delta\lambda$ against D at the two emission bands, which clearly show the linear relationships. The calculated n (1.59 at CNDPASDB, and 1.58 at Rh101 bands) are consistent with the intrinsic refractive index of the PS and PMMA, which indicates that the PL modulation in the Janus microsphere is attributed to the WGM-type resonance. The measured Q factors are on the order of 10^3 (Figure S8), which is pretty high for organic resonators. The size ratio between the two hemispherical parts was modulated to figure out the contribution of each part to the WGM resonance (Figure 2c). As shown in Figure S9, the value of $\lambda^2/\Delta\lambda$ measured from the CNDPASDB band are strikingly different from that at the Rh101 band, unless the size ratio is 1:1 (note that the refraction indices are approximately identical). Furthermore, as shown in Figure 2d-e, the $\lambda^2/\Delta\lambda$ values are linearly correlated to the diameter of corresponding hemispheres, rather than to that of the whole Janus particle. This demonstrates that the parallelly aligned hemispheres in the Janus structure form two independent WGM cavities, which is further confirmed by the numerical simulation (Figure S10).

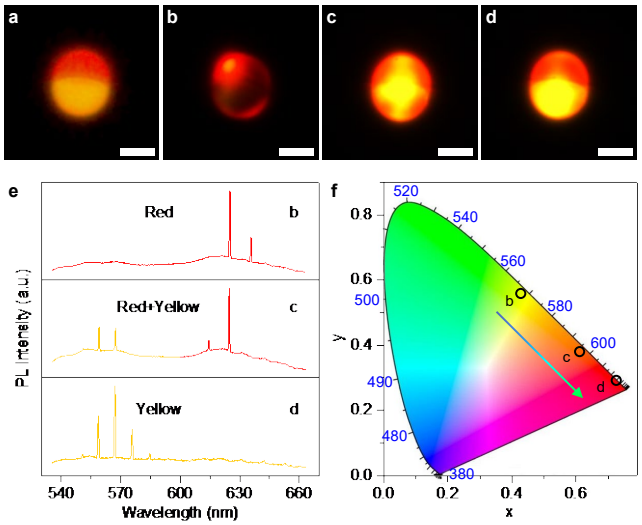

Figure 3. (a-d) PL images of the CNDPASDB-Rh101 doped Janus microsphere excited with UV light (a) and focused laser at different positions (b-d). Scale bars: 5 μm. (e) Lasing spectra of the CNDPASDB-Rh101 doped Janus microsphere excited at different positions shown in b-d. (f) Chromaticity of the lasing from b-d

This coupled cavity geometry enables to achieve color-tunable laser output from the Janus microsphere by pumping different segments. Figure 3a shows the PL image of a typical dual-color sphere with PS:PMMA ratio of ~1:1. By adjusting the excitation position, the output color was tuned from red to yellow (Figure 3b-e). Only the lasing emission from Rh101 was observed when the excitation was focused on the PMMA part, while the CNDPASDB lasing was achieved when the excitation moved onto the PS. Simultaneous dual-color lasing was obtained when the boundary of the two hemispheres was irradiated. Figure 3f shows the calculated chromaticity for the three lasing spectra, which exhibits a wide tuning range from yellow (0.42, 0.57) to red (0.71, 0.29).

The polarity driven encapsulation is universal to the hydrophilic and hydrophobic dye pairs; therefore, we can freely design the lasing color of the two hemispheres by doping with various dyes. As shown in Figure 4a-b, blue-pink colored Janus microspheres were obtained if we replace the doped dyes with cyano-substituted oligo(p-phenylenevinylene) (CNDPDSB) and sulforhodamine 101. The non-polar CNDPDSB molecules prefer to be embedded into the PS-rich hemispheres, while the ionic sulforhodamine 101 prefer to be incorporated into the PMMA. Under optical pumping, two separated sets of lasing were observed in the range of 449-474 and 606-631 nm (Figure 4c), consistent with the emissions of CNDPDSB and sulforhodamine 101, respectively (Figure S11). In a similar way, cyan-red and green-orange dual-color lasers were also successfully achieved from the coumarin 153-rhodamine 6G (Figure 4d-f), and coumarin 6-rhodamine B (Figure 4g-i) double-doped Janus microspheres. The corresponding chromaticity of the three dual-color lasing spectra was illustrated in Figure S12, displaying a wide tunable range covering the whole visible colors. This provides a general strategy for the programmable design and construction of compact all-color dual-wavelength lasers.

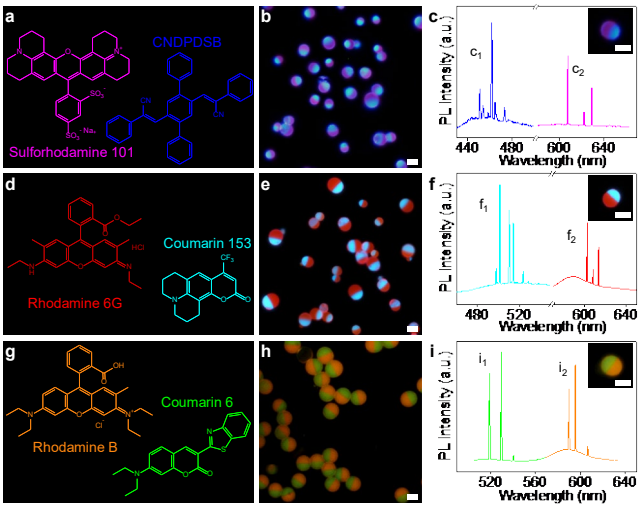

Figure 4. Molecular structures of sulforhodamine 101 and CNDPDSB (a); rhodamine 6G and coumarin 153 (d); rhodamine B and coumarin 6 (g). (b, e, h) PL images of the Janus microspheres doped with corresponding dyes. (c, f, i) Normalized lasing spectra of the Janus microspheres shown in the inset. Scale bars: 5 μm.

In summary, we developed a general approach to the synthesis of binary fluorescent organic Janus microspheres, which serve as side-by-side coupled WGM cavities for the achievement of dual-color microlasers. The connected WGM cavities can be separately modulated, offering the possibility to achieve novel photonic functionalities in the compact Janus structures. Moreover, the flexibility and compatibility of the Janus microspheres enable to flexibly design the lasing wavelength from the two hemispheres by doping with various dyes, demonstrating a general synthetic strategy for the dual-color microlasers across the full visible spectrum. We anticipate that our results will provide beneficial enlightenment for the design of multifunctional nanophotonic materials with novel performances and applications.

ASSOCIATED CONTENT

Supporting Information

Experimental details and additional data. The Supporting Information is available free of charge on the ACS Publications website.

AUTHOR INFORMATION

Corresponding Author

yszhao@iccas.ac.cn

Notes

The authors declare no competing financial interests.

ACKNOWLEDGMENT

This work was supported financially by the Ministry of Science and Technology of China (Grant No. 2017YFA0204502), and the National Natural Science Foundation of China (Grant Nos. 21790364, 21805246 and 21533013).

REFERENCES

(1) Bottanelli, F.; Kromann, E. B.; Allgeyer, E. S.; Erdmann, R. S.; Wood Baguley, S.; Sirinakis, G.; Schepartz, A.; Baddeley, D.; Toomre, D. K.; Rothman, J. E.; Bewersdorf, J. Two-colour live-cell nanoscale imaging of intracellular targets. *Nat. Commun.* **2016**, *7*, 10778.
(2) Kim, T.-H.; Cho, K.-S.; Lee, E. K.; Lee, S. J.; Chae, J.; Kim, J. W.; Kim, D. H.; Kwon, J.-Y.; Amaratunga, G.; Lee, S. Y.; Choi, B. L.; Kuk, Y.; Kim, J. M.; Kim, K. Full-colour quantum dot displays fabricated by transfer printing. *Nat. Photonics* **2011**, *5*, 176-182.
(3) Wang, D.; Yang, A.; Wang, W.; Hua, Y.; Schaller, R. D.; Schatz, G. C.; Odom, T. W. Band-edge engineering for controlled multi-modal nanolasing in plasmonic superlattices. *Nat. Nanotechnol.* **2017**, *12*, 889-894.
(4) Zhang, C.; Zou, C.-L.; Dong, H.; Yan, Y.; Yao, J.; Zhao, Y. S. Dual-color single-mode lasing in axially coupled organic nanowire resonators. *Sci. Adv.* **2017**, *3*, e1700225.
(5) Lv, Y.; Li, Y. J.; Li, J.; Yan, Y.; Yao, J.; Zhao, Y. S. All-color subwavelength output of organic flexible microlasers. *J. Am. Chem. Soc.* **2017**, *139*, 11329-11332.
(6) Okada, D.; Azzini, S.; Nishioka, H.; Ichimura, A.; Tsuji, H.; Nakamura, E.; Sasaki, F.; Genet, C.; Ebbesen, T. W.; Yamamoto, Y. π-Electronic co-crystal microcavities with selective vibronic-mode light amplification: Toward Förster resonance energy transfer lasing. *Nano Lett.* **2018**, *18*, 4396-4402.
(7) Ta, V. D.; Yang, S.; Wang, Y.; Gao, Y.; He, T.; Chen, R.; Demir, H. V.; Sun, H. Multicolor lasing prints. *Appl. Phys. Lett.* **2015**, *107*, 221103.
(8) Cerdán, L.; Enciso, E.; Martin, V.; Banuelos, J.; Lopez-Arbeloa, I.; Costela, A.; Garcia-Moreno, I. FRET-assisted laser emission in colloidal suspensions of dye-doped latex nanoparticles. *Nat. Photonics* **2012**, *6*, 621-626.
(9) Yang, Z.; Wang, D.; Meng, C.; Wu, Z.; Wang, Y.; Ma, Y.; Dai, L.; Liu, X.; Hasan, T.; Liu, X.; Yang, Q. Broadly defining lasing wavelengths in single bandgap-graded semiconductor nanowires. *Nano Lett.* **2014**, *14*, 3153-3159.
(10) Liu, Z.; Yin, L.; Ning, H.; Yang, Z.; Tong, L.; Ning, C.-Z. Dynamical color-controllable lasing with extremely wide tuning range from red to green in a single alloy nanowire using nanoscale manipulation. *Nano Lett.* **2013**, *13*, 4945-4950.
(11) Ning, C.-Z.; Dou, L.; Yang, P. Bandgap engineering in semiconductor alloy nanomaterials with widely tunable compositions. *Nat. Rev. Mater.* **2017**, *2*, 17070.
(12) Quochi, F.; Schwabegger, G.; Simbrunner, C.; Floris, F.; Saba, M.; Mura, A.; Sitter, H.; Bongiovanni, G. Extending the lasing wavelength coverage of organic semiconductor nanofibers by periodic organic–organic heteroepitaxy. *Adv. Opt. Mater.* **2013**, *1*, 117-122.
(13) Dou, L.; Lai, M.; Kley, C. S.; Yang, Y.; Bischak, C. G.; Zhang, D.; Eaton, S. W.; Ginsberg, N. S.; Yang, P. Spatially resolved multicolor $CsPbX_3$ nanowire heterojunctions via anion exchange. *Proc. Natl. Acad. Sci. U.S.A.* **2017**, *114*, 7216-7221.
(14) Fan, F.; Turkdogan, S.; Liu, Z.; Shelhammer, D.; Ning, C. Z. A monolithic white laser. *Nat. Nanotechnol.* **2015**, *10*, 796-803.
(15) Xu, J.; Ma, L.; Guo, P.; Zhuang, X.; Zhu, X.; Hu, W.; Duan, X.; Pan, A. Room-temperature dual-wavelength lasing from single-nanoribbon lateral heterostructures. *J. Am. Chem. Soc.* **2012**, *134*, 12394-12397.
(16) Zhuang, X.; Guo, P.; Zhang, Q.; Liu, H.; Li, D.; Hu, W.; Zhu, X.; Zhou, H.; Pan, A. Lateral composition-graded semiconductor nanoribbons for multi-color nanolasers. *Nano Res.* **2016**, *9*, 933-941.
(17) Walther, A.; Müller, A. H. E. Janus particles: Synthesis, self-assembly, physical properties, and applications. *Chem. Rev.* **2013**, *113*, 5194-5261.
(18) Chen, D.; Amstad, E.; Zhao, C.-X.; Cai, L.; Fan, J.; Chen, Q.; Hai, M.; Koehler, S.; Zhang, H.; Liang, F.; Yang, Z.; Weitz, D. A. Biocompatible amphiphilic hydrogel–solid dimer particles as colloidal surfactants. *ACS Nano* **2017**, *11*, 11978-11985.
(19) Hu, H. C.; Wu, L. Z.; Tan, Y. S.; Zhong, Q. X.; Chen, M.; Qiu, Y. H.; Yang, D.; Sun, B. Q.; Zhang, Q.; Yin, Y. D. Interfacial synthesis of highly stable $CsPbX_3$/oxide Janus nanoparticles. *J. Am. Chem. Soc.* **2018**, *140*, 406-412.
(20) Liang, F.; Zhang, C.; Yang, Z. Rational design and synthesis of Janus composites. *Adv. Mater.* **2014**, *26*, 6944-6949.

(21) Pang, X.; Wan, C.; Wang, M.; Lin, Z. Strictly biphasic soft and hard Janus structures: Synthesis, properties, and applications. *Angew. Chem. Int. Ed.* **2014**, *53*, 5524-5538.
(22) Wang, R.; Yu, B.; Jiang, X.; Yin, J. Understanding the host–guest interaction between responsive core-crosslinked hybrid nanoparticles of hyperbranched poly(ether amine) and dyes: The selective adsorption and smart separation of dyes in water. *Adv. Funct. Mater.* **2012**, *22*, 2606-2616.
(23) Choi, C.-H.; Weitz, D. A.; Lee, C.-S. One step formation of controllable complex emulsions: From functional particles to simultaneous encapsulation of hydrophilic and hydrophobic agents into desired position. *Adv. Mater.* **2013**, *25*, 2536-2541.
(24) Tobias, K.; Talha, G. M.; Christian, W.; Martin, S.; Stefan, R.; F., A. H.; F., B. S. A.; E., D. P. F.; Jan, R. B. "Sandwich" microcontact printing as a mild route towards monodisperse Janus particles with tailored bifunctionality. *Adv. Mater.* **2011**, *23*, 79-83.
(25) Yi, L. X.; Yee, P. I.; Canet, A.; Deniz, Y. M.; A., H. M.; Julius, V. G.; Jurriaan, H. Janus Particles with controllable patchiness and their chemical functionalization and supramolecular assembly. *Angew. Chem. Int. Ed.* **2009**, *48*, 7677-7682.
(26) Kuehne, A. J. C.; Gather, M. C. Organic lasers: Recent developments on materials, device geometries, and fabrication techniques. *Chem. Rev.* **2016**, *116*, 12823-12864.
(27) Hua, B.; Zhou, W.; Yang, Z. L.; Zhang, Z. H.; Shao, L.; Zhu, H. M.; Huang, F. H. Supramolecular solid-state microlaser constructed from pillar[5]arene-based host-guest complex microcrystals. *J. Am. Chem. Soc.* **2018**, *140*, 15651-15654.
(28) Zhu, G.; Huang, Z.; Xu, Z.; Yan, L.-T. Tailoring interfacial nanoparticle organization through entropy. *Acc. Chem. Res.* **2018**, *51*, 900-909.
(29) Ta, V. D.; Chen, R.; Sun, H. D. Self-assembled flexible microlasers. *Adv. Mater.* **2012**, *24*, OP60-OP64.
(30) Wei, C.; Gao, M.; Hu, F.; Yao, J.; Zhao, Y. S. Excimer emission in self-assembled organic spherical microstructures: An effective approach to wavelength switchable microlasers. *Adv. Opt. Mater.* **2016**, *4*, 1009-1014.
(31) Adachi, T.; Tong, L.; Kuwabara, J.; Kanbara, T.; Saeki, A.; Seki, S.; Yamamoto, Y. Spherical assemblies from π-conjugated alternating copolymers: Toward optoelectronic colloidal crystals. *J. Am. Chem. Soc.* **2013**, *135*, 870-876.
(32) Wei, C.; Liu, S.-Y.; Zou, C.-L.; Liu, Y.; Yao, J.; Zhao, Y. S. Controlled self-assembly of organic composite microdisks for efficient output coupling of whispering-gallery-mode lasers. *J. Am. Chem. Soc.* **2015**, *137*, 62-65.

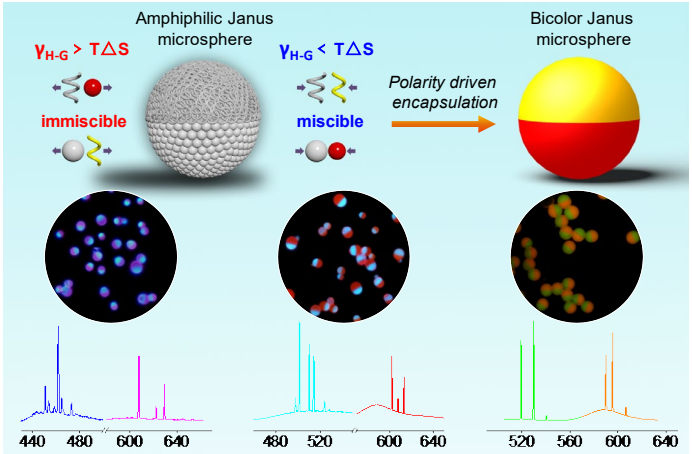
Amphiphilic Janus microsphere
Bicolor Janus microsphere
γH-G > TΔS
immiscible
γH-G < TΔS
miscible
Polarity driven encapsulation
440 480 600 640
480 520 600 640
520 560 600 640